

Theory of Crosslinked Bundles of Helical Filaments: Intrinsic Torques in Self-Limiting Biopolymer Assemblies

Claus Heussinger

*Georg-August-Universität Göttingen, Institut für Theoretische Physik,
Friedrich-Hund-Platz 1, 37077 Göttingen, Germany and*

Max Planck Institute for Dynamics and Self-Organization, Bunsenstr. 10, 37073 Göttingen, Germany

Gregory M. Grason

*Department of Polymer Science and Engineering,
University of Massachusetts, Amherst, MA 01003, USA*

Inspired by the complex influence of the globular crosslinking proteins on the formation of biofilament bundles in living organisms, we study and analyze a theoretical model for the structure and thermodynamics of bundles of helical filaments assembled in the presence of crosslinking molecules. The helical structure of filaments, a universal feature of biopolymers such as filamentous actin, is shown to generically frustrate the geometry of crosslinking between the “grooves” of two neighboring filaments. We develop a coarse-grained model to investigate the interplay between the geometry of binding and mechanics of both linker and filament distortion, and we show that crosslinking in parallel bundles of helical filaments generates *intrinsic torques*, of the type that tend to wind bundle superhelically about its central axis. Crosslinking mediates a non-linear competition between the preference for bundle twist and the size-dependent mechanical cost of filament bending, which in turn gives rise to feedback between the global twist of self-assembled bundles and their lateral size. Finally, we demonstrate that above a critical density of bound crosslinkers, twisted bundles form with a thermodynamically preferred radius that, in turn, increases with a further increase in crosslinking bonds. We identify the *stiffness* of crosslinking bonds as a key parameter governing the sensitivity of bundle structure and assembly to the availability and affinity of crosslinkers.

I. INTRODUCTION

Rope-like assemblies of filamentous biopolymers are important and common structural elements in living organisms. Fibers of cellulose and collagen provide mechanical reinforcement of extra-cellular plant and animal tissue [1] while inside of eukaryotic cells, bundles of cytoskeletal protein filaments – microtubules, filamentous actin (f-actin) and intermediate filaments – are implicated in an outstanding array of physiological processes, from cell division and adhesion to motility and mechanosensing [2]. Understanding the physical mechanisms that underly the robust and high fidelity assembly pathways of protein filaments is thus an important, outstanding challenge with broad implications in biology. Key questions revolve around the role played by the myriad types of relatively compact, crosslinking proteins that coassemble in parallel bundles and fibers of certain protein filaments, the primary example of these being parallel actin bundles [4, 5]. Though the intrinsic properties of f-actin are largely conserved among different cell types and species, the structural, mechanical and dynamic properties of f-actin bundles are evidently quite modular. For example, filopodial bundles [6, 7] that form at the periphery of motile cells are loosely organized and highly dynamical structures of rather limited diameter (~ 100 nm), while f-actin bundles formed in mechanosensory appendages of the cochlea and inner ear [18] are nearly crystalline in cross-section and quite large by comparison (~ 1 μ m). Recent experimental studies of parallel actin bundles *in vitro* [8–13] demonstrate that to large

extent the mechanical and structural properties of bundle assemblies can be attributed to the crosslinking proteins as well as their interactions with the bundled filaments.

An important but unresolved question concerns the organization of crosslinks in the bundle and how this organization reflects structural features of the filaments themselves. In particular, protein filaments are universally helical in structure [14], and by virtue of the helical distribution of binding sites, interactions mediated by proteins crosslinking neighboring filaments must reflect the underlying chiral nature of the assembly. Indeed, there is numerous experimental evidence to show that crosslinking actin in parallel bundles modifies the torsional state of constituent filaments from their native, unbound geometry [11–13, 15–18]. The extent to which this helical twist is transferred more globally to the structure of crosslinked actin bundles – as has been observed in superhelical assemblies of fibrin [19] and collagen fibers [20] – is presently unclear.

In this paper, we explore the fundamental interplay between the helical structure of biological protein filaments and intrinsic torques generated by self-organizing distributions of crosslinks between filaments in regular bundle arrays. Our task is to develop a generic theoretical model for the frustration that arises between the regular in-plane organization of filaments in bundles and the helical distribution of crosslinking sites along the filaments. We seek to understand how this frustration can be relieved at the expense of different types of mechanical distortions of the filament assembly, in particular, a global twist distortion of the parallel array. A num-

ber of theoretical [21–23], computational [24] and experimental [19] studies demonstrate that chiral filament interactions which tend to twist bundled assemblies have the important consequence of providing an intrinsic and thermodynamic limitation to the lateral growth of bundles. In the present study, we show that the helical distribution of crosslinking sites on the filaments gives rise to a tendency for neighboring filaments to twist in order to relieve the elastic cost of distorting crosslinks. In turn, the tendency to twist filaments superhelically in the bundle leads to a mechanical cost for growing the bundle diameter that for sufficiently weak crosslink affinities and sufficiently high crosslink densities becomes finite in equilibrium.

Our approach to this problem is based on a generalization of the “worm-like bundle” model of crosslinked filaments [25–27]. This semi-microscopic model treats filaments as semi-flexible polymers decorated by discrete arrays of sites to which elastic crosslinks between neighboring filaments bind. This model has been successfully used to analyze the complex mechanical response of crosslinked bundles to bend and twist deformations. However, it does not allow to explore the consequences of the helical filament structure for the bundle mechanical and thermodynamical properties.

In the present study, we consider a model where crosslink sites are located along helical “grooves” on the filaments, which are characterized by bending and torsional stiffness. Modeling the elastic cost of linker distortions, we show that crosslinking between helical filaments leads to an energetic preference to align the opposing grooves of crosslinked filaments. Depending on the relative stiffness of the linker and the filaments we find two different regimes: 1) a high-torque “groove-locked” regime, where stiff crosslinks force the grooves into alignment, and 2) a low-torque “groove-slip” regime, in which crosslinks are not stiff enough to enforce this alignment and cannot unwind the filaments from their native state of twist. Though of a distinct microscopic origin, we find that in the groove-locked regime linker-mediated interactions lead to a similar elastic frustration as occurring in “coiled-coil” assemblies of polypeptides [28]. Filament pairs may align opposing grooves by either untwisting the pitch of grooves themselves *or* by winding helically around one another with the appropriate pitch.

Based on the intrinsic and non-linear torques generated by crosslinking in helical filament bundles, our model makes two important predictions. First, we predict that subject to an external torque self-assembled bundles of crosslinked helical filaments exhibit non-linear torsional response that is highly-sensitive to both the intrinsic helical geometry of filaments as well as the fraction of bound crosslinks, ρ . Second, we show that the competition between the linker-generated torques and the mechanical energy of bending filaments in superhelical bundles gives rise to the formation of self-limited bundles when the crosslink fraction is larger than a critical value ρ_c , which is itself determined by the ratio of bending

cost of helically winding a pair of filaments to the torsional cost of unwinding the intrinsic twist of the helical grooves. A primary conclusion of this study is that finite-diameter bundles of helical filaments form preferentially when crosslinks are highly resistant to in-plane shear distortions and filaments have a large torsional stiffness relative to the bending modulus.

This article is organized as follows. In Sec. II we introduce our model of crosslinked helical filament assemblies and in Sec. III we derive the form of the linker-mediated torsional energy of filament bundles. In Sec. IV we determine the dependence of bundle twist on bundle size, as well as the torsional response of self-assembled bundles. In Sec. V we predict the thermodynamic behavior of crosslinked filament assemblies in terms of the density and binding energy of crosslinks in the bundle. Finally, we conclude with a discussion of our results in the context of biological filament assemblies.

II. MODEL OF CROSSLINKING IN HELICAL FILAMENT BUNDLES

A. Geometry of Crosslinked Helical Filament Bundles

To describe the interaction between crosslinking in parallel bundles and the helical geometry of constituent filaments, we introduce the following coarse-grained model, depicted schematically in Fig. 1. In the cross-section (“in-plane”), the bundle is organized into a hexagonal array, with the center-to-center spacing of neighbor filaments, d . Crosslinkers bind to neighboring filaments in parallel bundles, and reflecting the helical symmetry of the filament, the ends of crosslinks are located at discrete points on helical grooves on the filaments. In the most general case, helical filaments possess a range of groove geometries of differing helical symmetry. For the purposes of the following analysis, we focus on the simple case where binding sites are located on double-helical grooves, which are perfectly out of phase (180° between grooves). The crosslinking sites are linearly spaced by a vertical separation, σ^{-1} , along the filament backbone direction, and the pitch of each helical groove is defined to be $2\pi/\omega_0$.

Albeit simpler, this double helical geometry is not unlike the two-start helical structure of f-actin [29], whose grooves rotate at a rate $\omega_0 = 2\pi\sigma/13$ in the native state of twist and $\sigma^{-1} \simeq 5.7$ nm represents the vertical distance separating 2 actin monomers along the same bi-helical groove. While in actin filaments, the monomers on opposing grooves are off-set vertically by $\sigma/2$, the present simplified model has the advantage that in the lowest energy state, which allows for maximal crosslinking, all filaments maintain the same axial “orientation”, meaning that grooves in each vertical plane are aligned along the same direction. Certainly, the analysis may be extended to address groove geometries that lead to non-

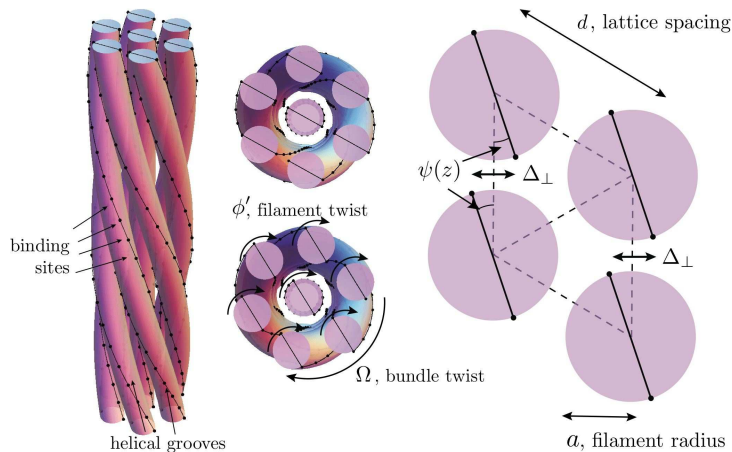


FIG. 1: Illustration of the bundle geometry. Filaments are arranged on the sites of a two-dimensional hexagonal lattice. Discrete crosslink binding sites are regularly spaced along the filament backbone, respecting the double-helical structure of the filaments. The binding sites on two neighboring filaments may be connected by crosslinkers. When bound, crosslink mediated torques act to align the binding sites on the two filaments. Alignment can be achieved, either by filament twist ϕ' , where filaments are untwisted from their native helical state, or by bundle twist, where filaments superhelically wind around the center of the bundle. Misaligned binding sites imply an elastic cost for the crosslinkers, which we parametrize in terms of the angle difference ψ with the optimal alignment and the associated “in-plane” shear deformation $\Delta_{\perp} \sim a\psi$.

trivial, inter-filament correlations, as has been done in ref. [30], but our purpose here is to analyze the simplest model describing the interplay between helical geometry of filaments and the inter- and intra-filament torques that arise in crosslinked parallel bundles.

In parallel bundles, crosslinks bind selectively to pairs of sites which are closest in separation (see Fig. 2), which in our model occur when grooves on any neighbor filament “cross”, and the orientation of the groove at a given plane is perfectly aligned with the in-plane vector separating the neighbors. For perfectly straight filaments with native twist, such a crossing occurs every π/ω_0 along the backbone between any neighbor pair, and over a distance $2\pi/(6\omega_0)$, the crossing rotates from one of the six neighbors of a given filament to the next. Here, we will consider the case where the fraction, ρ , of occupied crosslinking sites in the bulk of the bundle is fixed. By the assumption of the minimal crosslink stretching, crossing points are populated first, followed by sites closest to the crossing point, and so on, until a “binding zone” representing the 60° wedge shared by any 2 neighboring filaments is occupied with the appropriate number of crosslinks (see Fig. 2).

B. Mechanics of Crosslinks and Twist Geometry of Filaments and Bundle

To model the elastic cost of crosslinks that are poorly aligned due to the helical distribution of sites we intro-

duce the following simple crosslink energy,

$$E_{link} = -\epsilon + \frac{k_{\perp}}{2} \Delta_{\perp}^2. \quad (1)$$

Here, E_{link} is the energy of a single crosslinker in the bundle, and $-\epsilon$ represents the “bare” energy gain for binding between 2 perfectly aligned sites. The second term represents the elastic cost of *shear* distortions of crosslinks away from the perfectly aligned geometry perpendicular to the backbone orientations. Specifically, Δ_{\perp} represents the *in-plane shear* as shown in Fig. 1. This model has marked similarities with a model for contact between hydrophobic residues on α -helical polypeptide chains studied in ref. [31], and hence, our current model may also be applicable to the study of coiled-coil bundles of α -helices.

Depending on the location of the crosslink in the bundle, these distortions, Δ_{\perp} , are purely determined by the state of twist of constituent filaments as well as the global twisting of the bundle itself. The twist of individual filaments is described by the angle, $\phi(z)$, that describes the orientation of the groove in the $x-y$ plane of filament packing. Hence, for the case of native filament twist, $\phi' = \omega_0$. In addition to the “local” twist of individual filaments, the bundle may twist as a whole described by Ω , the rate at which in-plane lattice directions rotate around z axis, the long axis of the bundle. Notice that in this description, ϕ' and Ω are decoupled by construction, meaning that filaments may be twisted without the bundle experiencing twist ($\phi' \neq \omega_0$ and $\Omega = 0$) or the bundle may be twisted without distortion the native symmetry of the constituent filaments ($\phi' = \omega_0$ and $\Omega \neq 0$) [34]. It is clear from this geometry (Fig. 1) that Δ_{\perp} is determined by the *relative rotation* of the grooves with respect

to the bundle lattice directions. This relative rotation can be measured by the angle,

$$\psi(z) = \phi(z) - \Omega z \quad (2)$$

which gives the angle between the helical groove and the nearest neighbor lattice separation as shown in Fig. 1. From this we have the in-plane linker shear,

$$\Delta_{\perp} = 2a \sin \psi(z) \simeq 2a\psi(z). \quad (3)$$

When both ϕ' and Ω are non-zero, the distance between crossover points is determined by the distance over which the *relative angle* rotates by 60° . We will call this distance, ℓ , and refer to such a 60° wedge shared by 2 filaments as a “binding zone” (see Fig. 2). It is straightforward to see that,

$$\ell = \frac{\pi}{3\langle\psi'\rangle}, \quad (4)$$

where $\langle\psi'\rangle$ is the mean rate of relative rotation in this span. Likewise, it is easy to see that of this zone, only a length $\rho\ell$ centered around the crossover point will be occupied with crosslinks.

Before analyzing the structural and thermodynamic consequences of in-plane shear costs of crosslinking bonds, we note that a superhelical twist of the bundle introduces other, out-of-plane modes of crosslinker shear. We discuss, in the Appendix, that a reorganization of the crosslinking sites along the long axis of the bundle allows linkers to trade a high elastic energy out-of-plane shear cost for lower energy in-plane distortion. Furthermore, under this linker reorganization the elastic cost of non-zero out-of-plane shear, ultimately contributes to the total free energy of the bundle at higher order than the leading-order, $(\psi')^2$, cost of in-plane shear derived below and represents nominal modification to the forgoing analysis.

III. ELASTIC FREE ENERGY OF HELICAL FILAMENT BUNDLE TWIST

In this section, we consider a helical filament bundle at a fixed, constant rate of bundle twist, Ω . The aim is to integrate out the distribution of the individual crosslinks and the twist of filaments within a binding zone to derive an effective free energy in terms of bundle twist alone. From this, we learn that crosslinking helical filament bundles necessarily introduces intrinsic torques which tend to wind the bundle superhelically in order to reduce in-plane shearing of linkers.

Competing with the cost of crosslink shear, is the cost for twisting individual filaments away from their native helical symmetry,

$$E_{torsion} = \frac{C}{2} \int dz (\phi' - \omega_0)^2 = \frac{C}{2} \int dz \left[|\psi'|^2 - 2\psi'(\omega_0 - \Omega) + (\omega_0 - \Omega)^2 \right] \quad (5)$$

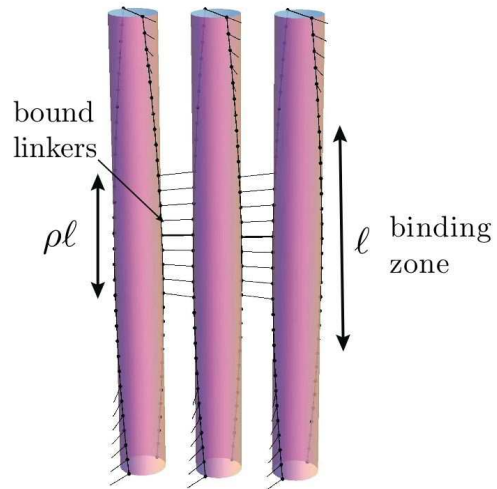


FIG. 2: The binding zone is defined as the length ℓ , over which the helical groove rotates by the angle $\pi/6$, which is the angle between two lattice directions in the hexagonal lattice. Crosslink sites are perfectly aligned, when the grooves of two neighboring filaments point towards each other, shown as a bold link in the figure. For a given linker density ρ , the optimal binding configuration is obtained, when crosslinks “fill-up” the binding zone starting from these aligned sites.

Here C is the torsional modulus of the filament and we used eq. (2) to rewrite the filament rotation, ϕ , in terms of the groove alignment angle ψ . We analyze the respective costs of linker shear and filament twist, by considering the profile of crosslinking occurring within a single binding zone (shown in Figure 2). Within a binding zone $\psi(z)$ rotates by 60° as opposing grooves come into near registry. Thus, if ℓ is the length of the binding zone along the long axis of the bundle, then the cross term in eq. (5) proportional to $\int_{-\ell/2}^{\ell/2} dz \psi' = \psi(+\ell/2) - \psi(-\ell/2) = \pi/3$ is fixed.

As shown in Fig. 2, at fixed fraction of bond crosslink sites, ρ , linkers occupy a span of size $\rho\ell$ centered around the close contact between opposing helical grooves. Hence, for ℓ fixed, we may write the ψ -dependence of the elastic energy of the binding zone (per filament) in terms of the following functional,

$$F(\ell) = \frac{1}{2} \int_{-\ell/2}^{\ell/2} dz \left[C|\psi'|^2 + \Gamma|\psi|^2 \theta(\rho\ell/2 - |z|) \right]. \quad (6)$$

where from eq. (3) we find that

$$\Gamma = 4k_{\perp} a^2 \sigma, \quad (7)$$

represents the effective pinning strength of the linkers located at $|z| \leq \rho\ell/2$, which favor pinning the relative orientation to $\psi = 0$. The minimal energy torsional state

of the filament is determined by,

$$C \frac{\partial^2 \psi}{\partial z^2} = \begin{cases} \Gamma \psi, & |z| \leq \rho \ell / 2 \\ 0, & |z| > \rho \ell / 2 \end{cases} \quad (8)$$

This equation, along with the boundary condition $\psi(\pm \ell / 2) = \pm \pi / 6$, is satisfied by the following rotation profile,

$$\psi(z) = \begin{cases} \psi_0 \sinh(\frac{z}{\lambda}), & |z| \leq \rho \ell / 2 \\ \psi_0 \cosh(\frac{\rho \ell}{2\lambda})(\frac{z - \rho \ell / 2}{\lambda}) + \psi_0 \sinh(\frac{\rho \ell}{2\lambda}), & |z| > \rho \ell / 2 \end{cases}, \quad (9)$$

where

$$\psi_0 = \frac{\pi / 6}{\cosh(\frac{\rho \ell}{2\lambda})(\frac{1 - \rho}{2\lambda}) + \sinh(\frac{\rho \ell}{2\lambda})}. \quad (10)$$

Here, $\lambda = \sqrt{C/\Gamma}$ is a characteristic lengthscale defined by the relative cost of filament twist and linker shear. It is the lengthscale over which the filament twist can adjust from its native rate to the value required in the binding zone.

The twist profile within a binding zone is largely determined by the ratio of this elastic lengthscale to the size of the binding zone. Some characteristic groove-slip profiles $\psi(z)$ are displayed in Figure 3. In the rigid filament limit, where $\ell/\lambda \ll 1$, the solution is simply $\psi(z) \simeq (\pi z/3\ell)$, which is equivalent to a homogeneously twisted state, $\phi' = \psi' + \Omega = \text{const}$. This indicates a weak modification of the filament twist due to crosslinker elasticity and we refer to this as the limit of *groove-slip*.

In the opposite, rigid-crosslink limit, when $\lambda \ll \rho \ell$, we can show that

$$\psi(z) \simeq \begin{cases} 0, & |z| \leq \rho \ell / 2 \\ \frac{\pi}{3} \frac{z - \rho \ell / 2}{\ell(1 - \rho)}, & |z| > \rho \ell / 2 \end{cases} \quad (11)$$

In this second situation, referred to as the *groove-locked* limit, the linker elasticity pins or locks the groove over the region of occupied linkers. As a consequence the filament twist in this region follows the bundle twist, $\phi' = \Omega$. The rotation of the groove towards the next binding partner is achieved over the reduced distance $(1 - \rho)\ell$, where there are no crosslinks. There, the filaments rotate freely according to a constant twist, $\phi' = \langle \psi' \rangle / (1 - \rho) + \Omega$. Accordingly, the filament twist energy will be minimized when $\Omega = \omega_0$ and $\langle \psi' \rangle = 0$. We find below that this twist profile results in a tendency to twist the bundle as a whole.

The minimal energy solution for $\psi(z)$, yields the following elastic energy for fixed ℓ ,

$$F(\ell)/\ell = \frac{\Gamma}{2} \left(\frac{\pi}{6} \right)^2 \frac{\sinh(\rho \bar{\ell})/\bar{\ell} + (1 - \rho) \cosh^2(\frac{\rho \bar{\ell}}{2})}{\left[\cosh(\frac{\rho \bar{\ell}}{2})\bar{\ell}(1 - \rho)/2 + \sinh(\frac{\rho \bar{\ell}}{2}) \right]^2}, \quad (12)$$

where $\bar{\ell} = \ell/\lambda$. Recalling that the mean rate of twist is related to the binding zone size by, $\langle \psi' \rangle = 2\pi/(6\ell)$, the

$F(\ell)/\ell$ has the following limits for groove-slip,

$$\lim_{\rho \bar{\ell} \ll 1} F(\ell)/\ell = \frac{C}{2} \langle \psi' \rangle^2 + \frac{\Gamma}{2} \left(\frac{\pi}{6} \right)^2 \frac{\rho^3}{3}, \quad (13)$$

and for groove-locked,

$$\lim_{\rho \bar{\ell} \gg 1} F(\ell)/\ell = \frac{C}{2} \frac{\langle \psi' \rangle^2}{(1 - \rho)}, \quad (14)$$

The physical interpretation underlying each limit is straightforward. In the groove-slip regime the elastic energy is computed from the homogeneous rotation profile, $\psi(z) = \langle \psi' \rangle z$ which incurs a torsional cost per unit length $\frac{C}{2} \langle \psi' \rangle^2$, as well as the cost of shearing the bound crosslinks according to $\Gamma \int_{-\rho \ell / 2}^{\rho \ell / 2} dz |\langle \psi' \rangle z|^2 \propto \langle \psi' \rangle^2 (\rho \ell)^3 \propto \rho^3 \ell$. In the groove-locked regime, $\psi = 0$ where crosslinks are bound and the $\pi/3$ rotation is carried over the unbound length, $(1 - \rho)\ell$, of the binding zone for which $\psi' = \langle \psi' \rangle / (1 - \rho)$. Hence, the mean torsional energy of eq. (14).

The final step in minimizing the elastic energy over the filament torsion is accomplished by minimizing the combined elastic and torsional energy density over ℓ for fixed Ω to find the dependence of linker-mediated groove interactions on bundle twist,

$$f_{twist}(\Omega) = \min_{\ell} \left[F(\ell)/\ell - C \langle \psi' \rangle (\omega_0 - \Omega) + \frac{C}{2} (\omega_0 - \Omega)^2 \right]. \quad (15)$$

In the limits described above it is straightforward to show,

$$\langle \psi' \rangle_* \simeq \begin{cases} \omega_0 - \Omega, & \rho \ell_* \ll \lambda \\ (\omega_0 - \Omega)(1 - \rho), & \rho \ell_* \gg \lambda \end{cases} \quad (16)$$

where again, $\ell_* = \pi/3 \langle \psi' \rangle_*$. The second-line above shows the clear preference of the groove-locked regime to maintain contact between crosslinked and nearly parallel grooves on neighbor filaments over large distances, $\ell_* \rightarrow \infty$, as $\rho \rightarrow 1$. Inserting these limiting cases into eq. (15) we find a central result of our analysis, the free energy of linker and filament elasticity in terms of Ω ,

$$f_{twist}(\Omega) \simeq \begin{cases} \frac{\Gamma}{2} \left(\frac{\pi}{6} \right)^2 \frac{\rho^3}{3}, & \rho \ell_* \ll \lambda \\ \rho \frac{C}{2} (\Omega - \omega_0)^2, & \rho \ell_* \gg \lambda \end{cases} \quad (17)$$

The full non-linear behavior for the coarse-grained free energy (as calculated from eq. (15)) is shown in Figure 4. In the groove-slip limit ($\rho \ell_* \ll \lambda$) the linker-mediated groove interactions become insensitive to bundle twist, as the crosslinks are not stiff enough to noticeably affect the state of twist of the individual filaments. In this case, the elastic energy is set by the deformation of the flexible crosslinks, $f_{twist} \sim \Gamma$, but does not depend on the amplitude of the bundle twist Ω . Thus, increasing bundle twist does not appreciably increase the cost of shear deformation in the crosslinks. Instead, the crosslinks reorganize into new binding sites allowing them to maintain a

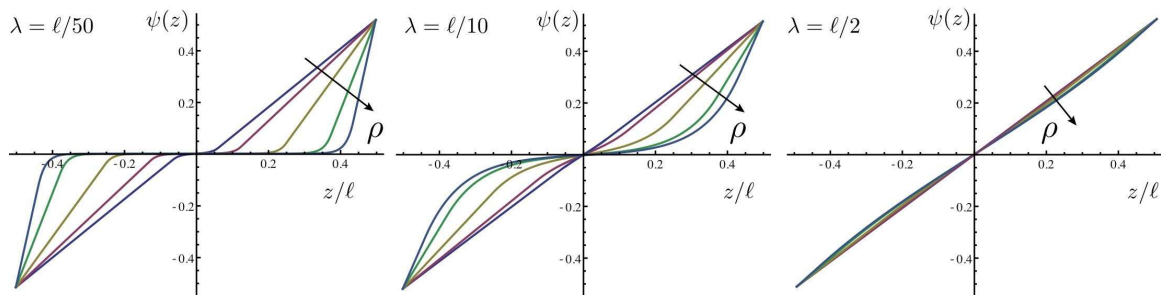


FIG. 3: Plots of groove-slip profile for three different groove-slip lengths λ and a range of bound linker fractions: $\rho = 0.125, 0.25, 0.5, 0.75$ and 0.875 . (Left) limit of groove-locked, (center) intermediate and (right) limit of groove-slip.

constant average crosslink deformation. This is possible, as in hexagonal bundles the angle $\psi = 2\pi/3$ is an upper limit for the angle between two neighboring grooves, *independent* of the size of the binding zone, ℓ . Accordingly, the shear deformation $\Delta_{\perp} = 2a\psi$ of the maximally stretched linker cannot grow larger than $2a\rho\pi/3$, independent of the bundle twist Ω .

In the groove-locked limit ($\rho\ell_* \gg \lambda$) the energy scale is set by the filament twist stiffness C . The linker-mediated interactions lead to a preference to twist the bundle at a rate equal to the intrinsic twist of filaments, $\Omega \sim \omega_0$. This latter case reflects the fact that crosslinks on neighboring filaments lock a span of length $\rho\ell$ into a parallel configuration. By rotating the interfilament position at a rate $\Omega = \omega_0$, these groove-locked domains on neighbor filaments can be brought into coincidence with the native, helical geometry of the untwisted grooves. Therefore, a high degree of crosslinking by rigid linkers ($\rho\ell_* \gg 1$) induces an *intrinsic torque* on the entire bundle, which prefers the filament lattice to rotate at the rate of the helical grooves. The crossover between groove-locked and groove-slip behavior can be related to $\delta\Omega = \Omega - \omega_0$. Groove-locking occurs for $|\delta\Omega| \lesssim \delta\Omega_c$, while groove-slip occurs for larger deviations from optimal twist, $|\delta\Omega|$, where,

$$\delta\Omega_c \equiv \rho \frac{\pi}{6\sqrt{3}\lambda}. \quad (18)$$

Therefore, as shown in Fig. 4, the harmonic, linear-elastic twist dependence of the linker elastic energy is maintained for bundle twists near to the intrinsic rate of groove twist, ω_0 , over range of twists that increases with the fraction of bound crosslinks.

IV. PROPERTIES OF BUNDLES WITH CROSSLINK INDUCED TORQUE

In the previous section we have derived the form of the linker-induced elastic energy for global twist of crosslinked bundles of helical filaments. We found that crosslinks induce torques that tend to twist the bundle as a whole. These intrinsic torques give rise to unusual

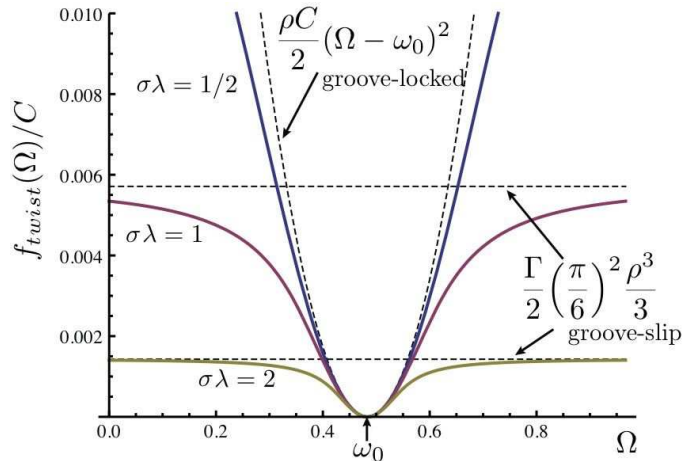


FIG. 4: Coarse-grained elastic free energy $f_{twist}(\Omega)$ as determined from eq. (eq:fgroove). The limiting forms of groove-locked and groove-slip are indicated as dashed lines.

structural and mechanical properties for self-assembled bundles, including a highly non-linear dependence of bundle twist on lateral size and externally applied torsional moment.

To demonstrate these properties, we consider crosslinked bundles of semi-flexible helical filaments with a twist-dependence described by eq. (15). The additional mechanical costs of filament bending can be described by the following simple elastic energy,

$$E_{bend} = \frac{K}{2} \sum_i \int ds \kappa^2(\mathbf{r}_i). \quad (19)$$

where K is the bend modulus and $\kappa \simeq \Omega^2 |\mathbf{r}_i|$ is the curvature of the i th filament in a twisted bundle. Averaging over a cylindrical cross-section of radius R , we obtain a free energy per unit filament length,

$$f(\Omega) = f_{twist}(\Omega) + \frac{K}{4} \Omega^4 R^2. \quad (20)$$

Analytical progress is hampered by the complicated form of the twist free energy, Eq. (15). In the following

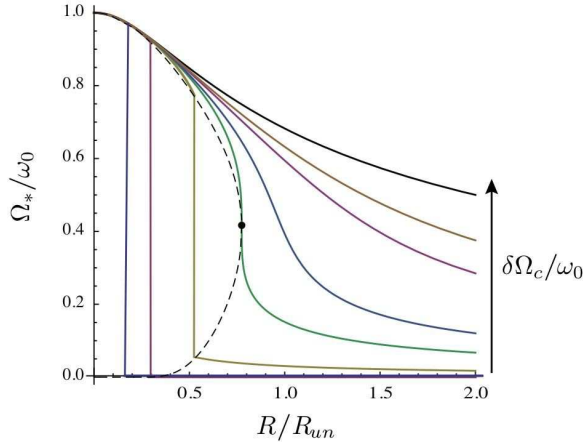


FIG. 5: Plots of the equilibrium degree of bundle twist, Ω_* , vs. bundle twist, R , for $\delta\Omega_c/\omega_0 = 0.1, 0.2, 0.3, \delta\bar{\Omega}_c \simeq 0.362, 0.4, 0.5, 0.6$ and ∞ , the groove-locked limit described by eq. (25). The filled circle shows a critical point at $\delta\bar{\Omega}_c \simeq 0.362$, $\bar{\Omega}_* \simeq 0.407$ and $\bar{R} = 1.073$, while the dashed line shows region of first-order jumps in Ω_* for $\delta\bar{\Omega}_c < 0.362$.

we therefore assume the simplified expression

$$f_{twist}(\Omega) = \frac{\rho C \delta\Omega_c^2}{2} \left[1 - e^{-(\Omega - \omega_0)^2 / \delta\Omega_c^2} \right], \quad (21)$$

which captures the limiting groove-locked and groove-slip behaviors of eq. (17) as well as the overall non-linear dependence on Ω between these two limits.

In the following subsection, we analyze the structural and mechanical properties of bundles in terms of two dimensionless parameters, $\bar{R} \equiv R/R_{un}$ and $\delta\bar{\Omega}_c \equiv \delta\Omega_c/\omega_0$, where

$$R_{un} = \sqrt{\frac{\rho C}{K\omega_0^2}}, \quad (22)$$

is a characteristic bundle size at which the mechanical cost of filament bending becomes comparable to the linker-induced cost of twisting the filaments from their native symmetry.

A. Size dependent bundle twist

We first analyze the equilibrium twist of self-assembled bundles as function of lateral radius, R . According to $f_{twist}(\Omega)$ crosslink-mediated torques prefer a constant degree of twist, $\Omega = \omega_0$. On the other hand, bending resistance of filaments penalizes bundle twist in an R -dependent manner due to the linear increase of filament curvature with radial distance from the helical bundle center.

Based on our expression for $f_{twist}(\Omega)$, For a fixed R and ρ , the equilibrium bundle twist is determined from the solutions to

$$(\rho C)^{-1} \frac{\partial f}{\partial \Omega} = (\bar{\Omega} - 1) e^{-(\bar{\Omega} - 1)^2 / \delta\bar{\Omega}_c^2} + \bar{\Omega}^3 \bar{R}^2 = 0. \quad (23)$$

where $\bar{\Omega} \equiv \Omega/\omega_0$ is the reduced twist. For the limiting case of $\delta\bar{\Omega}_c \gg 1$, where linker shear is sufficiently strong to maintain the high torque, groove-locked behavior over the entire range $0 \leq \bar{\Omega} \leq 1$, the equilibrium bundle twist satisfies a cubic equation,

$$(\bar{\Omega} - 1) + \bar{\Omega}^3 \bar{R}^2 = 0, \text{ for } \delta\bar{\Omega}_c \gg 1. \quad (24)$$

In this limit, the R dependence of the twist has the form

$$\bar{\Omega}(\bar{R}) = \frac{1}{\sqrt{3}\bar{R}} \left[x^{1/3}(\bar{R}) - x^{-1/3}(\bar{R}) \right], \text{ for } \delta\bar{\Omega}_c \gg 1, \quad (25)$$

where

$$x(\bar{R}) = \sqrt{\frac{27}{4}\bar{R}} + \sqrt{1 + \frac{27\bar{R}^2}{4}}. \quad (26)$$

In this groove-locked limit, the bundle is unwound continuously as R increases due to the increased cost of filament bending. In the limit of large bundles, $\bar{R} \gg 1$, eq. (25) predicts a power law dependence of optimal twist on bundle size, $\bar{\Omega}_* \sim \bar{R}^{-2/3}$.

The range of groove-locked behavior is highly sensitive to the degree of crosslinking as $\delta\Omega_c \propto \rho$, hence for weakly crosslinked bundles as $\rho \rightarrow 0$ the torsional energy dependence necessarily crosses over to groove-slip behavior, becoming largely insensitive to Ω . Thus, in the most general case, we expect the groove-locked predictions of Ω_* described by eq. (25) to hold only for sufficiently small bundles where the groove-locked approximation predicts that $1 - \bar{\Omega}_*(\bar{R}) \lesssim \delta\bar{\Omega}_c$. Beyond this size, we expect the decrease of Ω_* with increasing size R to become more rapid as the bundle slips from the high-torque region.

The full dependence of Ω_* vs. R is shown in Fig. 5 for several values of $\delta\bar{\Omega}_c < 1$. These show that unwinding of the bundle due to the increased bending cost of large bundles becomes more rapid in comparison to the predictions of eq. (25) as $\delta\bar{\Omega}_c$ is decreased. For a critical value, $\delta\bar{\Omega}_c = \sqrt{\frac{11\sqrt{33}}{32} - \frac{59}{32}} \simeq 0.362$, the sensitivity of twist to bundle size becomes singular, $\frac{\delta\Omega_*}{\delta R} \rightarrow -\infty$, at $\bar{R} \simeq 1.0731$. For $\delta\bar{\Omega}_c$ below this critical value, Ω_* unwinds by a discontinuous, first-order jump, as the elastic energy minimum slips from the narrow high-torque behavior near $\Omega \approx \omega_0$ to the low-torque, groove-slip behavior of $f_{twist}(\Omega)$ for $\omega_0 - \Omega \lesssim \delta\Omega_c$.

In this regime, the equilibrium state of twist is therefore highly susceptible to small changes in the mechanical or geometrical properties of the bundle. Changing only slightly bundle radius or crosslink density may result in a sudden and strong reduction of the overall bundle twist $\bar{\Omega}$.

B. Crosslinked bundles of helical filaments subject to external torque

In this section, we demonstrate how this sensitivity leads to a highly non-linear twist response when the

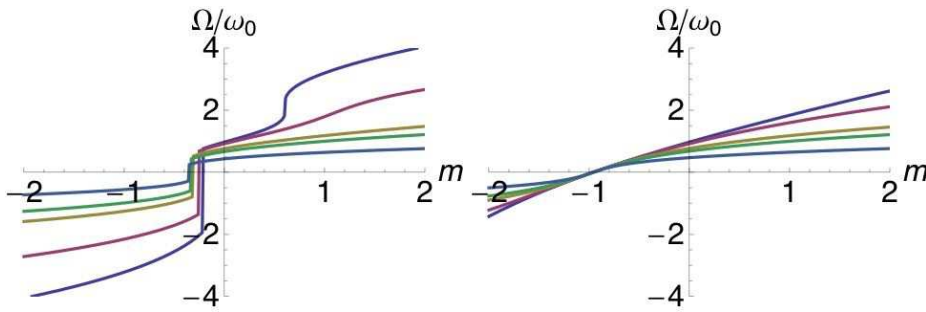


FIG. 6: Bundle twist Ω as a function of reduced torque $m = M/\rho C\omega_0$, for different $\bar{R}^2 = 0.03, 0.1, 0.5, 1.0, 5.0$. (left) A small value of $\delta\bar{\Omega}_c = 1$ allows to observe the discontinuous transition from groove-locked to slip as the external torque is increased. (right) For a larger value of $\delta\bar{\Omega}_c = 5$ the torque-twist relation is completely smooth.

bundle is subject to an external torque. Experiments that probe the torque-twist relation of single molecules have proven fruitful tools in advancing the understanding of the mechanical properties of biopolymers, such as DNA [32]. While the active manipulation of filament bundles is still a very delicate task [33], experiments in this direction may soon be feasible and may therefore provide an indirect means to probe the elastic properties of crosslinkers and their interactions with filaments.

In the presence of an external torque M , the free energy Eq. (20) becomes

$$f(\Omega) = f_{\text{twist}}(\Omega) + \frac{K}{4}\Omega^4 R^2 - M\Omega. \quad (27)$$

In the absence of the filament bending term $\sim K\Omega^4$, it is straightforward to see that the bundle is thermodynamically unstable for any nonzero value of M . The linear term $-M\Omega$ leads to a tilting of the twist free energy $f_{\text{twist}}(\Omega)$. As f_{twist} is asymptotically independent of Ω , in the absence of bending resistance, the thermodynamic groundstate is always the fully twisted state, $\Omega \rightarrow \infty$. Physically, this means that increasing the external torque does not lead to restoring forces, e.g. in the form of crosslink shearing. Instead, the bundle adapts to the increased load by a reorganization of the crosslinks into new binding sites.

Accounting for the mechanical cost of filament bending, the bundle is stabilized at a value of Ω , at which the twist-induced bending energy of the filaments balance the external torque. The full dependence of Ω vs. M is shown in Fig. 6. For small values of $\delta\bar{\Omega}_c$ and \bar{R} the instability appears as a sudden change of Ω with the external torque M . Note that due to the helical nature of the filaments, the response of the bundle will be inherently asymmetric and different for positive or negative torques. Hence, careful measurements of the non-linear torsional response of the self-assembled bundles should provide an indirect, experimental means to probe the twist state of crosslinked filaments.

V. LINKER-MEDIATED FILAMENT ASSEMBLY

In the previous sections we have discussed the properties of bundles of a given radius R . In this section we analyze the equilibrium thermodynamics of a system of self-assembled filaments and consider the thermodynamic stability of bundles of finite radius in the presence of a fixed degree of crosslinking.

Here, we consider a system possessing a fixed total number of filaments. In the bundled state, all filaments are assumed to form bundles of a mean-size, R , and a negligible number of unbundled filaments remain dispersed in solution. As described in eq. (1), each bound crosslink contributes, $-\epsilon$, of cohesive free energy. In the bulk of a self-assembled aggregate, crosslinks contribute $-3\rho\epsilon\sigma$ per unit filament length, as there are 3 crosslinking “channels” per filament in the interior of the bundle. At the outer boundary of the bundle, there are fewer crosslinks, roughly $3/2\rho\sigma L$ fewer cohesive bonds times the number of filaments at the surface of the bundle, N_s . For a large bundle with a circular cross-section, we may estimate $N_s \simeq 2\pi R/d$ so that the net cohesive free energy per unit filament length from crosslinked bundle of size R has the form,

$$F_{\text{coh}}/N_f L = -3\rho\epsilon\sigma + \frac{3\rho\sigma\epsilon}{\rho_0 d R}, \quad (28)$$

where $\rho_0 = d^{-2}/\sqrt{3}$. Combining the cohesive energy with the elastic costs of linker shear and filament bending we may write the total free energy per unit filament length,

$$f(\Omega, R) = f_{\text{twist}}(\Omega) + \frac{\rho C \omega_0^2}{2} \left[\frac{\Omega^4 R^2 (\rho_c/\rho)}{2\omega_0^4 d^2} + \frac{(\epsilon/\epsilon_c)}{d\rho_0 R} - \epsilon/\epsilon_c \right] \quad (29)$$

where the ratio of bend to twist moduli define a characteristic crosslink fraction,

$$\rho_c = \frac{K(\omega_0 d)^2}{C}, \quad (30)$$

and

$$\epsilon_c = \frac{C\omega_0^2}{6\sigma}, \quad (31)$$

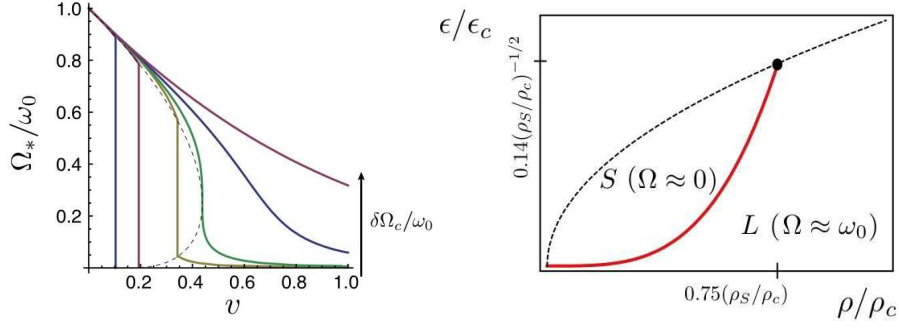


FIG. 7: (left) Bundle twist Ω in thermodynamic equilibrium as function of v for various value of $\rho_S/\rho = 0, 1, 1.333, 1.5, 2, 3$. (right) A sketch of the resulting phase diagram indicating the discontinuous transition from groove-locked (L) to groove-slip (S). The critical point shifts along the dashed line, when the effective stiffness of crosslinks, as characterized by ρ_S/ρ_c is changed.

is a characteristic cohesive energy scale. The thermodynamics of filament assembly are characterized by the dependence of the equilibrium, free energy minimizing values of R and Ω on ρ and ϵ . It is straightforward to show that the value of R minimizing $f(\Omega, R)$ at fixed Ω is determined by a balance between the cohesive and bending energies of the bundle, satisfying

$$R_*^3(\Omega) = \frac{d}{\rho_0(\Omega/\omega_0)^4}(\epsilon/\epsilon_c)(\rho/\rho_c). \quad (32)$$

Thus, the growth of equilibrium radius is quite generally correlated to decreasing twist for self-assembled bundles, and a non-zero measure of bundle twist implies a finite equilibrium radius.

Using the definition of $\delta\Omega_c$, Eq.(18), we can define another characteristic crosslink fraction,

$$\rho_S \equiv \frac{\omega_0\rho}{\delta\Omega_c} = \frac{6\sqrt{3}}{\pi}\omega_0\lambda \quad (33)$$

that characterizes the crosslink density below which the bundle “slips” to the low-torque elastic energy at $\Omega = 0$. With the solution for R_* , Eq. (32), and the form of f_{twist} from eq. (21), we may rewrite the reduced energy density purely in terms of the reduced twist, $\bar{\Omega}$,

$$\frac{f(\bar{\Omega})}{\rho C \omega_0^2} = \frac{(\rho/\rho_S)^2}{2} \left[1 - e^{-(\bar{\Omega}-1)^2/(\rho/\rho_S)^2} \right] + \frac{3}{4} v(\rho, \epsilon) \bar{\Omega}^{4/3} - \epsilon/\epsilon_c, \quad (34)$$

where,

$$v(\rho, \epsilon) \equiv 3^{1/3} \frac{(\epsilon/\epsilon_c)^{2/3}}{(\rho/\rho_c)^{1/3}}. \quad (35)$$

The reduced form of the free energy density, eq. (34), demonstrates that the phase behavior of helical crosslinked bundles is determined by two dimensionless parameters: ρ/ρ_S and v . Consequently the thermodynamic dependence of the assembly on crosslink density and cohesive energy of crosslinks is encoded in the ρ and ϵ dependence of these parameters.

The first term in eq. (34), representing the crosslink-mediated torsional energy, is minimized at $\bar{\Omega} = 1$, while the second term, representing the combined cohesive and bending energies is minimized at zero twist, $\bar{\Omega} = 0$. Hence, generically $f(\bar{\Omega})$ may be characterized by two minima, whose relative depth is determined by ρ/ρ_S and v . It is straightforward to analyze the case of rigid linkers, for which we expect $\rho/\rho_S \gg 1$ over the range of filament assembly and where the first term in eq. (34) adopts the groove-locked limit, $(\bar{\Omega}-1)^2/2$. In this case, we minimize the reduced free energy density for the limiting cases,

$$\bar{\Omega}_* \simeq \begin{cases} 1 - v, & \text{for } v \ll 1 \text{ and } \rho \gg \rho_S \\ v^{-3}, & \text{for } v \gg 1 \text{ and } \rho \gg \rho_S \end{cases} \quad (36)$$

we note that in the limit of $v \ll 1$ and $\rho/\rho_S \gg 1$ the minimum of $f(\bar{\Omega})$ corresponds to the groove-locked state, $\bar{\Omega}_* \rightarrow 1$ from which we find the following dependence of equilibrium bundle size on ρ and ϵ ,

$$R_* \simeq d \begin{cases} (\epsilon/\epsilon_c)^{1/3}(\rho/\rho_c)^{1/3}, & \text{for } v \ll 1 \text{ and } \rho \gg \rho_S \\ 3(\epsilon/\epsilon_c)^3(\rho/\rho_c)^{-1}, & \text{for } v \gg 1 \text{ and } \rho \gg \rho_S \end{cases}, \quad (37)$$

where we have used $(d/\rho_0)^{1/3} \approx d$. Stable, microscopic bundles are associated with the limit of high crosslink density and relatively weak cohesive energy per link where $v \ll 1$ while $\rho \gg \rho_S$. As one might have expected, eq. (37) suggests that due to the adhesive effect of crosslinking, bundles grow with increasing ϵ , as larger bundles imply smaller surface effects. Perhaps more surprising, the $v \ll 1$ limit of this model predicts that at large linker densities bundles assemble to a finite size that grows with increasing fraction of bound crosslinkers, growing as $R_* \sim \rho^{1/3}$. In this regime the bundle is fully twisted, so filaments have to bend in order to be incorporated into the bundle. Increasing bundle size is therefore only possible when the mechanical cost of filament bending is offset by the cohesive energy gain of adding crosslinks.

In the limit of large v , note that the size of equilibrium bundles also diverges in the limit of small linker fraction

as $R_* \sim \rho^{-1}$, indicating a smooth crossover to a state of unlimited, macroscopic filament assembly in the $\rho \rightarrow 0$ limit.

It is straightforward to determine the full equation of state for an arbitrary value of ρ_S , relating equilibrium twist, $\bar{\Omega}_*$, to ρ and ϵ from $df/d\bar{\Omega} = 0$,

$$\left(\frac{\rho}{\rho_S}\right)^2 = -\frac{(1 - \bar{\Omega}_*)^2}{\ln[v\bar{\Omega}_*^{1/3}/(1 - \bar{\Omega}_*)]}. \quad (38)$$

The solutions to this equation of state are shown in Fig. 7, where we plot Ω_* as a function of v for constant values of ρ/ρ_S . These results show that equilibrium twist decreases from ω_0 both with *decreased* ρ/ρ_S as well as with *increased* v . Underlying the unwinding of equilibrium bundles are two effects, driven by decreasing crosslink fraction. First, as the number of crosslinkers in the bundles is reduced, the strength of the intrinsic torques that drive the bundle towards $\Omega_* = 1$ is correspondingly reduced. Second, v diverges as $\rho \rightarrow 0$ indicating a dramatic increase in the relative importance of filament bending in the elastic energy, further enhancing the preference to untwist the bundle. According to eq. (32) equilibrium bundles grow in radius as they unwind, and ultimately diverge in size at the untwisted, $\Omega = 0$ state.

Fig. 7 shows this unwinding with decreased ρ may occur either continuously or discontinuously, accompanied by a rapid jump in equilibrium twist. From the equation of state, Eq. (38), we find a critical value $v = v_* = 3/2^{4/3}e \simeq 0.438$ that separates smooth from discontinuous bundle untwisting. At this critical point, $\rho_*/\rho_S = 3/4, \Omega_* = 1/4$ [35]. For $v < v_*$ the equilibrium twist state jumps from the groove-locked minimum of $f(\bar{\Omega})$ near $\Omega = \omega_0$ to the nearly unwound groove-slip state. This discontinuous and highly non-linear thermodynamic dependence of self-assembled bundles derives from the non-linear interplay between linker shear and filament twist encoded in $f_{twist}(\Omega)$.

We now proceed to sketch the possible phase diagrams of self-assembled filament systems. We begin by analyzing a transition between the 2 torsional states of self-assembled filament arrays, groove-locked vs. groove-slip. In terms of parameters ϵ and ρ we sketch the twist-state phase diagram of Fig.7b. Thermodynamically stable finite-sized bundles are associated with the groove-locked regime (L), while in the slip regime (S) radial bundle growth is nearly unlimited in equilibrium as $\Omega_* \approx 0$. The line of discontinuous transitions between locked and slip regime terminates at the critical point. The transition line can approximately be calculated by comparing the $\Omega \rightarrow \omega_0$ solution ($f/(C\rho\omega_0^2) \rightarrow 3v/4 - \epsilon/\epsilon_c$, groove-locked) with the $\Omega \rightarrow 0$ solution ($f/(C\rho\omega_0^2) \rightarrow (\rho/\rho_S)^2/2 - \epsilon/\epsilon_c$, groove-slip). Note, that this calculation will not be accurate close to the critical point, where $\Omega_* \approx \omega_0/4$. Equating these two limiting forms of the energy, we find a relationship between ϵ and ρ , satisfied at the (LS) boundary,

$$\epsilon_{(LS)}/\epsilon_c \simeq (2/3)^{3/2}(\rho/\rho_c)^{7/2}(\rho_c/\rho_S)^3 \quad (LS). \quad (39)$$

Across this line of first order transitions, the equilibrium twist of bundles slips from a nearly groove-locked state with $\Omega \approx \omega_0$ of microscopic size to a nearly untwisted and macroscopically sized bundle.

The location of the critical point follows from the condition $v = v_* \approx 0.438$ which gives

$$\epsilon/\epsilon_c = v_*^{3/2}(\rho/\rho_c)^{1/2}. \quad (40)$$

This critical branch is sketched as a dashed line in Fig. 7b. Hence, with increasing ρ_S , say by decreasing linker shear stiffness, the (LS) boundary and the critical point shift to larger values of ρ . Notice that the bundle phase diagram has the familiar form of a liquid-gas transition. Stable finite-sized bundles correspond to the ‘‘condensed’’ phase, while in the ‘‘gas-phase’’ the bundles are large and nearly untwisted. Below a critical value of ϵ corresponding to v_* , there is a well-defined first-order transition between these states at a certain linker density. For sufficiently strong cohesive energies the state of untwisted, macroscopic assembly evolves continuously to the state of finite-sized bundles at high linker fraction.

In addition to the ‘‘microscopic’’ and ‘‘macroscopic’’ bundle phases, we also consider the possibility of a state of unassembled filaments, where no bundles form and filaments remain uncrosslinked. Neglecting entropic contributions, such as translational entropy of linkers and filaments, the free energy density in the filament phase vanishes, $f_{fil} = 0$, as free filaments are mechanically undistorted. Thus, the state of bundled filaments is stable with respect to unbundled filaments where the free energy of Eq.(29) remains negative, indicating a net lowering of the free energy due to crosslink binding. The phase boundary, $f(\Omega_*, R_*) = 0$, can be determined approximately by assuming the limiting cases of groove-locked ($\Omega = \omega_0$) and groove-slip ($\Omega = 0$). Equating the energy density of the groove-locked bundles to the free filament case, we find the condition satisfied along the twisted, bundle/filament (BF) phase boundary,

$$\epsilon_{(BF)}/\epsilon_c \simeq \frac{81}{64}(\rho/\rho_c)^{-1}. \quad (41)$$

We may also estimate the phase boundary between untwisted, macroscopic bundle assembly and free filament phase, denoted as (UF), by comparing the free energy of the state with $\Omega = 0$ and $R \rightarrow \infty$ to the free filament energy in both the groove-locked and groove-slip regimes. From eq. (34), we find this boundary satisfies,

$$\epsilon_{(UF)}/\epsilon_c \simeq \begin{cases} \frac{1}{2}(\rho/\rho_S)^2 & \text{for } \rho \ll \rho_S \\ \frac{1}{2} & \text{for } \rho \gg \rho_S \end{cases}. \quad (42)$$

Based on the ϵ - and ρ -dependence of these boundaries, we sketch two basic scenarios for the diagram of state of bundle assembly of crosslinked helical filaments, based on the interference of the (LS), (BF) and (UF) boundaries. When $\rho_S < 2.53\rho_c$, the critical point at v_* and ρ_* lies deep within the filament phase and the (LS) line is not

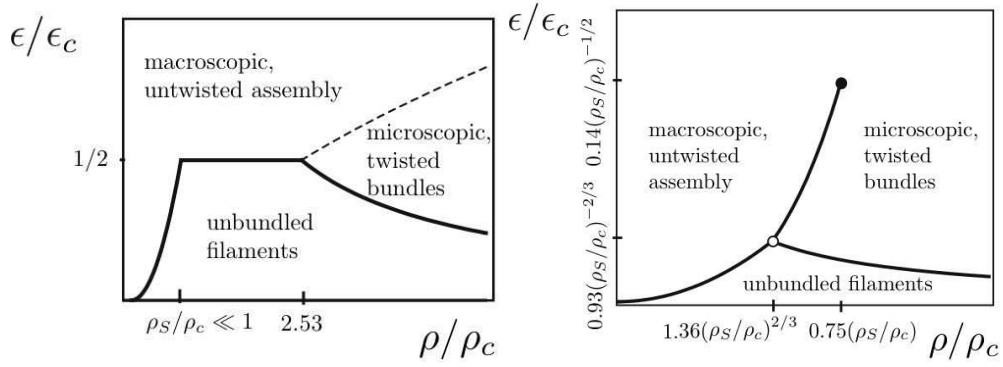


FIG. 8: Sketches of the two scenarios for the state diagram of bundle assembly in the $\epsilon - \rho$ plane: rigid linkers, $\rho_c/\rho_S \gg 1$ (left); and flexible linkers, $\rho_c/\rho_S \ll 1$ (right). For $\rho_S < 2.53\rho_c$ the critical point is not relevant as it would lie deep inside the filament phase (left). The dashed line indicates the crossover between microscopic, finite-sized bundles and macroscopic bundles with diverging size. (right) For $\rho_S > 2.53\rho_c$ the critical point (ρ_*, ϵ_*) is inside the bundle phase (shown as filled circle). The triple point (ρ_T, ϵ_T) signals coexistence of the filament and the two assembled filament phases (shown as open circle).

relevant. This is the limit of effectively *rigid linkers*, characterized by $\rho_c/\rho_S \gg 1$. We sketch the phase behavior in Fig. 8a. Here, the boundaries (UF) and (BF) meet at the point $\epsilon = \epsilon_c/2$ and $\rho = 81/32\rho_c \simeq 2.53\rho_c$. Below this critical value of cohesive energy of crosslinks, $\epsilon_c/2$, bundles only form at crosslinker fractions that are larger than $1.27\rho_c(\epsilon_c/\epsilon)$. Bundles formed for this low-cohesive energy regime are twisted and grow in size with increasing crosslinking density as $R_* \sim \rho^{1/3}$. For smaller crosslink densities, the filaments remain in the dispersed state, allowing for a narrow region of slip-induced, macroscopic filament assembly predicted for $\rho \lesssim \rho_S$. For $\epsilon > \epsilon_c/2$ filaments assemble at all crosslinker fractions, with a state of macroscopic bundle assembly crossing over to microscopic, twisted bundles as ρ increase from 0 to values of order ρ_c .

The second scenario, $\rho_S \geq 2.53\rho_c$, occurs in the limit of *flexible linkers*. In this case the critical point lies inside the regime of linker-mediated filament assembly, as shown in Fig. 8b. In addition to the line of first-order transitions separating the groove-locked and groove-slip states of bundles, we also have a triple point, at which the two bundle phases, macroscopic and microscopic, coexist with the state of dispersed filaments. From the scaling expressions given for (BF) and (UF) we locate the triple point at

$$\rho_T/\rho_c \simeq 1.36(\rho_S/\rho_c)^{2/3}, \quad \epsilon_T/\epsilon \simeq 0.93(\rho_S/\rho_c)^{-2/3}. \quad (43)$$

In this case, bundled phases form for all cohesive energies, $\epsilon > \epsilon_T$, with a line of first-order transitions that separates the phase of macroscopic, nearly untwisted bundles at low linker densities from the phase of small radius, twisted bundles at high linker density and terminates at the second order critical point. For weaker cohesive energy per crosslinker, there are three possible states of filament assembly. At low density of bound linkers, $\rho < \rho_{(\text{UF})}$, we predict a phase of untwisted, macroscopic filament assembly. For intermediate densities of linkers,

$\rho_{(\text{UF})} < \rho < \rho_{(\text{BF})}$, we predict a state of unbound and disperse linkers. Finally, at the highest densities of linkers, $\rho > \rho_{(\text{BF})}$, we find a re-entrant state of twisted, filament bundles, whose finite diameter grows with linker density as $R_* \sim \rho^{1/3}$.

VI. CONCLUSION

In this study, we have analyzed a coarse-grained model for crosslinking in ordered arrays, or bundles, of helical filaments. A primary result of this model is a quantitative relationship between the presence of crosslinkers in bundles, and intrinsic torques that act to coherently twist entire bundles superhelically around their central axis. Such global distortion naturally competes with the mechanical cost of bending stiff filaments, providing a complex feedback between the torsional structure, size and thermodynamics of bundle assembly. Along with the total number and binding affinity of crosslinkers, the key parameters governing the structure and assembly of crosslinked bundles include the elastic properties of the filaments and the linkers themselves. Indeed, we find the ratio $\lambda = \sqrt{C/\Gamma}$ of linker stiffness Γ to filament stiffness C to be particularly important for controlling not only the structure and properties of self-assembled bundles, but also the sensitivity of these properties – size, twist and stability – to changes in the availability and affinity of crosslinkers.

The effective torsional elastic energy of bundles derived in Sec. III describes an intrinsic frustration between shear distortion of crosslinks that bind together neighboring filament grooves and the torsional elastic response of filaments themselves. In the limiting case of perfectly rigid linkers, where $\lambda \rightarrow 0$, our model is not unlike the elastic model of coiled-coils of Neukirch, Gorieli and Hausrath [28], in which adhesive interactions between neighboring helical molecules maintain grooves in

perfect registry. Geometrically, this can be accomplished either by untwisting the rotation of the grooves or by superhelically twisting the filaments about the bundle axis. The twist elastic energy of the filaments is minimal for the state of perfect superhelical twist, $\Omega = \omega_0$. Deviations from this optimal geometry, while maintaining perfect groove contact, are described by a coarse-grained twist free-energy cost, $f_{twist} = \rho C(\Omega - \omega_0)^2/2$.

Our theory generalizes the coiled-coil model of perfect groove contact in two ways. First, grooves only maintain contact over fraction, ρ , of the length of the filaments due to the finite density of crosslinkers between any filament pair. This distinction accounts for the ρ dependence of the effective torsional modulus, ρC of the stiff-linker regime, a significant effect in the context of linker-mediated assembly.

The second important and novel effect captured by the model is the elastic compliance of the linker bonds themselves. Flexibility of bound linkers gives rise to highly nonlinear torsional properties of the bundles themselves. The twist elastic behavior predicted by the case of groove-locked contact, gives way to a highly-twist compliant state (“groove-slip”) when deviations from the optimal twist geometry are large, $|\Omega - \omega_0| \gtrsim \delta\Omega_c$. The crossover twist $\delta\Omega_c \sim \rho/\lambda$, which delineates the groove-locked from the groove-slip regime, increases both with increased linker density, ρ and increased linker stiffness Γ . Hence, untwisting bundles out of the groove-locked into the groove-slip state indicates a shift in the mechanical load from filament twist to in-plane crosslink shear distortions. In this limit the elastic cost is insensitive to bundle twist Ω , and given by $f_{twist} = \rho C \delta\Omega_c^2/2 \simeq \rho^3 \Gamma$.

The distinction between a purely harmonic twist energy for stiff linkers and a non-linear twist energy for flexible linkers has key consequences for the structural and mechanical properties of crosslinked, helical filament bundles. This is reflected in the optimal rate of bundle twist, a property that is determined not only by a balance of the cost of linker shear and filament twist, but also the mechanical costs associated with filament bend. The costs of filament bending are themselves highly sensitive to the lateral radius of the bundle due to the increased curvature of filaments away from the bundle center [23]. In the case of rigid linkers grooves remain locked in close contact, so that the optimal twist derives purely from the competition between the bending cost of rotating filaments superhelically in the bundle, and the twist elastic cost needed to maintain groove-alignment when filaments are parallel. This balance is described by the results of eq. (25), where the increased cost of bending filaments in large bundles leads to a continuous unwind as $\Omega \sim R^{-2/3}$.

In contrast, bundles bound by relatively flexible linkers are much more sensitive to bundle size, the sensitivity ultimately becoming singular when $\delta\Omega_c \leq 0.362\omega_0$. These flexibly crosslinked bundles exhibit a discontinuous drop in Ω as a function of R , as the bundle rapidly jumps between the groove-locked and groove-slip behav-

iors. Hence, in this flexible linker regime, the unwinding of bundle twist with increased size is largely determined by a competition between filament bending and linker shear due to misaligned grooves. A similar distinction is predicted for the non-linear torsional response of bundles: Ω depends continuously on externally applied torque for rigidly crosslinked bundles; while flexibly crosslinked bundles are multi-stable, exhibiting discontinuous transitions between groove-locked and groove-slip states driven by external torque.

These non-linear structural and mechanical properties reflect the frustration of the geometry of crosslinking within helical filament bundles that ultimately gives rise to intrinsic mechanical torques that lead to *self-limiting bundle assembly*. Considering the thermodynamically optimal state of twist and radius for a system of associating filaments and linkers, we found two basic scenarios for the dependence of assembly behavior on the number and affinity of crosslinkers, as parameterized by ρ and ϵ , respectively. For the case of *rigid linkers* (shown in Fig. 8a), we find that assembled filaments maintain the high-torque, groove-locked state over the relevant range of their assembly. Above a critical cohesive energy per crosslinker, $\epsilon_c/2$, we predict that filament assemblies form at all linker densities, with macroscopically large and untwisted assembly behavior at low ρ crossing over continuously to a regime of twisted and finite sized bundles at large ρ . For less cohesive crosslinking bonds, $\epsilon < \epsilon_c/2$, we find that filaments remain largely unbundled below a linker density $\rho \lesssim \rho_c$, above which they form twisted bundles whose lateral size grows as $R_* \sim \rho^{1/3}$. For bundles crosslinked by *flexible linkers* (behavior shown in Fig. 8a) the transition between highly and weakly twisted states as function of increased ρ is discontinuous below a critical value of ϵ . We also find that finite-sized bundles, untwisted macroscopic assemblies and unbundled, free filaments coexist at a triple point whose precise location is sensitive to the flexibility of linkers as parameterized by ρ_S . For values of ϵ below this triple point, we predict that macroscopic assembly occurs in the limit of small ρ , giving way to a dispersed filament phase at intermediate ρ -values and at the highest range of linker density, a re-entrant phase of finite-sized linker mediated bundles occurs.

The rich spectrum of possible assembly behavior can be fully classified in terms of three parameters. The fundamental cohesive energy scale is determined by $\epsilon_c \propto C\omega_0^2\sigma^{-1}$, which corresponds to the energy of untwisting the intrinsic rotation of the helical grooves of the filaments. The different modes of elastic deformation induced by crosslinkers in helical filament bundles account for the presence of two fundamental scales of bound crosslinker fraction, ρ . The first, $\rho_c \propto K(\omega_0 d)^2/C$, can be understood as the ratio of the mechanical costs of two pair-wise filament geometries: $K\omega_0^4 d^2$, roughly the bend cost of winding a filament pair into a groove-locked coiled-coil geometry; and $C\omega_0^2$, the mechanical cost of untwisting the intrinsic helical grooves into par-

allel filaments. We find that for flexible crosslinks, ρ_c sets a lower limit for the fraction of bound crosslinkers at which self-limited bundles form, suggesting that self-assembled bundles are thermodynamically favored when the cost of filament bend is relatively small compared to the cost of filament twisting. The final parameter, $\rho_S \propto \lambda\omega_0 \propto (\Gamma/C)^{1/2}\omega_0$, reflects the relative elastic cost of linker shear to filament twist and determines the density of crosslinkers below which high-torque, groove-locked bundle states crossover to low-torque, groove-slip behavior. Hence, we can classify the thermodynamic distinctions between linker-mediated assembly by the ratio ρ_c/ρ_S which is much greater or less than 1 for the respective rigid and flexible behaviors depicted in Fig. 8.

The predictions of our coarse-grained model are most directly relevant to the formation of parallel actin bundles [3], self-organized cytoskeletal filament assemblies that form in a variety of cellular specializations under the influence of compact crosslinking proteins [4–6]. There is a range of experimental evidence of parallel actin bundles formed *in vivo* [15–18] and *in vitro* [11–13] showing that the presence of certain crosslinking proteins affects the torsional state of bundled filaments, leading to a modest adjustment of the rotation rate of primary helix formed by the actin monomers. Recent small-angle scattering studies suggest, in fact, that the presence of different crosslinking proteins modify the twist of bundle actin filaments to a similar degree, but reconstituted solutions of actin bundles exhibit a remarkably different sensitivity to the concentration of crosslinking proteins [13]. The crosslinking protein fascin, a primary component of filopodial bundles [6], was shown to assemble filaments into bundles with a continuously variable degree of filament twist, while the crosslinking protein espin [5], an abundant crosslinker in microvillar and mechanosensitive stereociliar bundles, drove a discrete transition between the native state of twist and the torsional geometry of the “fully-bundled” actin filaments. Theoretical studies of a model actin filaments in bulk, parallel arrays attribute this difference in twist sensitivity to differences in the *stiffness* of the crosslinking bonds themselves [13, 30].

In our model, we show that the presence of crosslinking bonds in parallel arrays of helical filaments not only modifies the torsional geometry of individual filaments, but in general determines the amount of global twist of the entire bundle assembly. In particular, we show that the competition between the inter-filament geometry preferred by crosslinking and the bend elasticity of filaments mediates an intrinsic feedback between the lateral assembly size and the amount of superhelical twist. An important and general prediction of our model is the appearance of a thermodynamically stable phase of finite radius bundles at sufficiently high crosslink fractions that exhibits a linker dependent equilibrium radius, $R_* \sim \rho^{1/3}$. Claessens *et al* has explored the dependence of actin bundles formed in reconstituted solutions of filaments and the crosslinker, fascin [11]. Above a critical ratio of fascin to actin monomer, r , they found that the mean diame-

ter of bundles formed exhibited a powerlaw dependence, $R_* \sim r^{0.3}$, for small bundles, consistent with the predictions our coarse-grained model, which predict that the radius of twisted bundles grows with bound linker fractions as $R_* \sim \rho^{1/3}$. Hence, our model establishes a thermodynamic link between simultaneous influence of crosslinker fraction on bundle size and degree of filament twist in these actin/fascin experiments. Additionally, our theory establishes a range of further predictions on both the affinity and flexibility of crosslinking proteins, suggesting the need for further experiments on the influence of size and structure of parallel actin bundles on properties of crosslinkers. Notably, the implied differences in the compliance between fascin and espin crosslinks should be correlated with measurably differences in the assembly thermodynamics of reconstituted bundle forming solutions.

In summary, we have found that although crosslinking bonds between helical filaments mediate net cohesive interactions between filaments, the complex interplay between the mechanics of linker and filament distortions ultimately gives rise to a nontrivial dependence of the structure of self-assembled bundles on the number of bound linkers. We quantitatively model the thermodynamic influence of a number of microscopic parameters, from filament stiffness and intrinsic twist to the affinity of crosslink bonds. Among these, we show that the stiffness of the linkers themselves account for remarkable differences in the sensitivity of bundle structure to the availability of crosslinks. It is natural to expect that living systems may exploit the intrinsic frustration of crosslinking in helical filament bundles as robust means of regulating the size and structure of self-assembled bundles, not by modifying properties of the filaments, but instead by carefully regulating the number and type of crosslinking proteins alone.

Acknowledgments

The authors would like to acknowledge H. Shin for useful comments, and the hospitality of the Aspen Center for Physics, where this study originated. CH was supported by a Feodor Lynen fellowship of the German Humboldt Foundation. GG was supported by the NSF Career program under DMR Grant 09-55760.

Appendix A: Out-of-plane shear

In this appendix we demonstrate how out-of-plane shear deformations of crosslinkers may partially relax through a coupling to in-plane shear modes. Generalizing eq.(1) we consider an energy of crosslinking,

$$E_{link} = -\epsilon + \frac{k_{\perp}}{2}\Delta_{\perp}^2 + \frac{k_{\parallel}}{2}\Delta_{\parallel}^2, \quad (A1)$$

that contains, next to the in-plane shear deformations, Δ_{\perp} , the out-of plane shear, Δ_{\parallel} , which can be associated with filaments tilting into the plane of lattice order. In a twisted bundle, filaments are increasingly tilted along the azimuthal direction as the radial distance from the bundle center increases,

$$\hat{\mathbf{t}}(\mathbf{r}) \simeq \hat{z} + \Omega \hat{z} \times \mathbf{r}, \quad (\text{A2})$$

where \mathbf{r} is the radial vector from the center of the bundle. The in-plane distance between crosslinking points is fixed to $a' = d - 2a$, and we can relate the out-of-plane shear to the average tilt angle, θ_{ij} , of two neighboring filaments

$$\Delta_{\parallel} = 2a' \sin \theta_{ij} = 2a' \hat{\mathbf{t}} \cdot \hat{\mathbf{r}}_{ij} = 2a' \Omega (\hat{z} \times \mathbf{r}) \cdot \hat{\mathbf{r}}_{ij} \quad (\text{A3})$$

where \mathbf{r} in this equation refers to the mean in-plane position of filaments i and j and $\hat{\mathbf{r}}_{ij}$ is a unit vector that points from one filament to the other. Hence, in the twisted geometry, out-of-plane shear depends on $|\hat{\mathbf{r}}_{ij} \times \mathbf{r}|$, and is different for different filament pairs in the bundle. As we are interested in Δ_{\parallel}^2 , we can replace $|\hat{\mathbf{r}}_{ij} \times \mathbf{r}|^2$ with its average over the 6-fold nearest neighbor directions on the hexagonal lattice, $\langle |\hat{\mathbf{r}}_{ij} \times \mathbf{r}|^2 \rangle = r^2/2$ and the neighbor-averaged shear becomes,

$$\langle \Delta_{\parallel}^2 \rangle = 2a'^2 (\Omega r)^2. \quad (\text{A4})$$

Notice that this shear is insensitive to $\phi(z)$, unlike Δ_{\perp} .

As described in eq. (A3), out-of-plane shearing occurs when neighboring filaments, say $+$ and $-$, sharing crosslinks, tilt along their nearest neighbor separation vector, $\hat{\mathbf{r}}_{+-}$, making an angle θ_0 , relative to the straight configuration as shown in Fig. 9.

This assumes the crosslinks to bind in the “horizontal” $x - y$ plane, which is perpendicular to the bundle axis. However, if we allow the crosslinks to relax their binding geometry at fixed ρ after shear takes place, then the actual shear angle of the crosslinks θ , may be reduced from the shear angle of the crosslinks, θ_0 . This proceeds by shifting the linker ends bound to the $+$ ($-$) filament “upstream” (“downstream”), by an amount $\delta z_+ = \delta/2$ ($\delta z_- = \delta/2$) and reduces the out of plane shear to $\Delta_{\parallel} = a' \theta_0 - \delta$.

The amount of linker shift, δ , is determined from the competing effect of in-plane shear. Due to the rotation of the filament groove, as described by ψ' , the shift of crosslink ends *also* alters the in-plane shear angle to $\psi + \psi' \delta$, where we assume that the rotation profile for both filaments is identical. Integrating the in-plane shear along one binding zone from $z = -\rho\ell$ to $z = +\rho\ell$ and noting from the analysis of Sec.III that $\psi(z) = -\psi(z)$ while $\psi'(z) = \psi'(-z)$, the elastic contribution per unit length from out of plane shear from a single-binding zone can be written as,

$$E_{\parallel}(\delta)/L = \frac{\Gamma \rho}{8} \delta^2 \langle \psi'^2 \rangle_{\rho} + \frac{\rho \Gamma'}{2} \left(\theta_0 - \frac{\delta}{a'} \right)^2, \quad (\text{A5})$$

where

$$\langle \psi'^2 \rangle_{\rho} \equiv \frac{\int_{-\rho\ell}^{\rho\ell} dz \psi'(z)}{\rho\ell}, \quad (\text{A6})$$

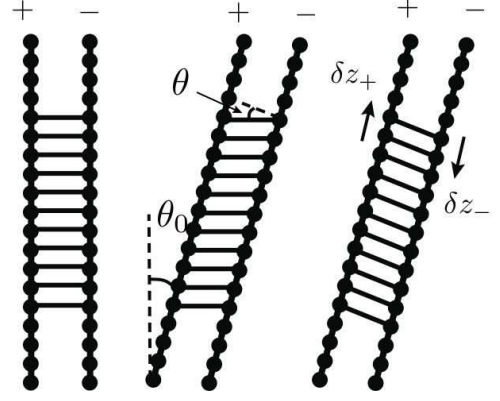


FIG. 9: A schematic of linker binding reorganization in response to an out-of-plane shear cost for 2 filaments grooves labeled “ $+$ ” and “ $-$ ”. Linkers are sheared with respect to the filament backbones by angle, θ , when a filament pair tilts along the direction of nearest neighbor separation, as shown in the middle. The shifting the bound ends of linkers up- and down-stream respectively from the $+$ and $-$ filaments, the links may relax the shear angle made with respect to the filament from the tilt angle, θ_{+-} , as shown on the right.

and $\Gamma' = k_{\parallel} a'^2 \sigma$. Minimizing over the shift of bound linker ends we find,

$$\delta_*/a' = \theta_0 \frac{\Gamma'}{\Gamma' + \Gamma a'^2/4}, \quad (\text{A7})$$

and an effective free energy contribution per unit length of the interfilament groove,

$$E_{\parallel}/L = \frac{\rho}{2} \theta_0^2 \langle \psi'^2 \rangle_{\rho} \frac{\Gamma \Gamma' a'^2}{4\Gamma' + \Gamma \langle \psi'^2 \rangle_{\rho} a'^2}. \quad (\text{A8})$$

Thus, we find that the coupling between out-of-plane and in-plane shear modes leads to a tilt-dependence renormalization of the torsional energy of the filaments ($\sim C \langle \psi'^2 \rangle_{\rho}$).

In the limit that linkers are softer to out-of-plane shear than to in-plane shear, or $\Gamma' \ll \Gamma$, the contribution to the bundle energy from the out-of-plane shear is clear negligible compared to the in-plane cost. From eq. (A8) we find that also in the limit that $\Gamma' \gg \Gamma$, the out-of-plane shear leads to a renormalization of the effective twist modulus of filaments, $C_{eff} = C + \rho(\Omega r)^2 \Gamma a'^2/16$, using $\langle \theta_0^2 \rangle = (\Omega r)^2/2$. Relative to the effective energy analyzed in Sec.IV and V, the net correction to the linker mediated-twist energy of the bundle from out-of-plane shear mode ultimately represents a higher-order term in Ω , proportional to $\Omega^2(\Omega - \omega_0)^2$, and therefore, will not strongly alter the quantitative analysis of bundle thermodynamics from the $\Gamma' = 0$ case.

-
- [1] P. Fratzl, *Cur. Opin. Coll. Int. Sci.* **8**, 32 (2003).
- [2] S. M. Rafelski and J. A. Theriot, *Ann. Rev. Biochem.* **73**, 209 (2004).
- [3] C. Revenu, R. Athman, S. Robine, and D. Louvard, *Nat. Rev. Mole. Cell Biol.* **5**, 635 (2004).
- [4] T. D. Pollard and J. A. Cooper, *Ann. Rev. Biochem.* **55**, 987 (1986).
- [5] J. R. Bartles, *Curr. Opin. Cell Biol.* **2**, 72 (2000).
- [6] J. Faix and K. Rottner, *Curr. Opin. Cell Biol.* **18**, 18 (2006).
- [7] Y. S. Aratyn, T. E. Schaus, E. W. Taylor, and G. G. Borisy, *Mol. Biol. Cell.* **18**, 3928 (2007).
- [8] J. H. Shin, L. Mahadevan, P. T. So and P. Matsudaira, *J. Mol. Biol.* **337** 255 (2004).
- [9] J. H. Shin, M. Gardel, L. Mahadevan, P. Matsudaira and D. A. Weitz, *Proc. Nat. Acad. Sci. USA* **101** 9636 (2004).
- [10] M. M. A. E. Claessens, M. Bathe, E. Frey, and A. R. Bausch, *Nat. Materials* **5**, 748 (2008).
- [11] M. M. A. E. Claessens, C. Semmrich, L. Ramos, and A. R. Bausch, *Proc. Natl. Acad. Sci. USA* **105**, 8819 (2008).
- [12] K. R. Purdy, J. R. Bartles, and G. C. L. Wong. 2007, *Phys. Rev. Lett.* **98** 058105 (2007).
- [13] H. Shin, K. R. Purdy, J. R. Bartles, G. C. L. Wong, and G. M. Grason, *Phys. Rev. Lett.* **103** 238102 (2009).
- [14] J. M. Squire and P. J. Vibert, eds. *Fibrous Protein Structure* (Academic Press, London, 1987).
- [15] D. J. DeRosier and R. Censullo, *J. Mol. Biol.* **146**, 77 (1981).
- [16] L. G. Tilney, D. J. DeRosier and M. J. Mulroy, *J. Cell Biol.* **86**, 244 (1980).
- [17] D. J. DeRosier and L. G. Tilney, *Cold Spring Harb. Symp. Quant. Biol.* **46**, 525 (1982).
- [18] L. G. Tilney, E. H. Egelman, D. J. DeRosier and J. C. Saunders, *J. Cell. Biol.* **96**, 822 (1983).
- [19] J. W. Weisel, C. Nagaswami and L. Makowski, *Proc. Nat. Acad. Sci. USA* **84**, 8991 (1987).
- [20] V. Ottani, D. Martinin, M. Franchi, A. Ruggeri and M. Raspanti, *Micron* **33**, 587 (2002).
- [21] M. S. Turner, R. W. Briehl, F. A. Ferrone and R. Josephs, *Phys. Rev. Lett.* **90**, 128103 (2003).
- [22] G. M. Grason and R. F. Bruinsma, *Phys. Rev. Lett.* **99**, 098101 (2007).
- [23] G. M. Grason, *Phys. Rev. E* **79**, 041919 (2009).
- [24] Y. Yang, R. B. Meyer and M. F. Hagan, *Phys. Rev. Lett.* **104**, 258102 (2010).
- [25] M. Bathe, C. Heussinger, M.M.A.E Claessens, A. Bausch and E. Frey, *Biophys. J.* **94**, 2955 (2008).
- [26] C. Heussinger, M. Bathe, E. Frey, *Phys. Rev. Lett.* **99**, 048101 (2007).
- [27] C. Heussinger, F. Schüller and E. Frey, *Phys. Rev. E* **81**, 021904 (2010).
- [28] S. Neukirch, A. Goriely and A. C. Hausrath, *Phys. Rev. Lett.* **100**, 038105 (2008).
- [29] K. Holmes, D. Popp, W. Gebhard and W. Kabsch, *Nature* **347**, 44(1990).
- [30] H. Shin and G. M. Grason, *Phys. Rev. E* **82**, 051919 (2010).
- [31] O. N. Yagurtcu, C. W. Wolgemuth and S. X. Sun, *Biophys. J.* **99**, 3892 (2010).
- [32] P. Nelson, *Biophys. J.* **74**, 2501 (1998).
- [33] D. Strehle *et al.*, *Eur. Biophys. J.* **40**, 93 (2011).
- [34] Strictly speaking, bundle twist and the rotation of helical grooves are coupled geometrically, since even for $\phi' = 0$, when $\Omega \neq 0$ the writhe of helically bent filament backbones will lead to precession of groove orientation in the $x - y$ plane of linker binding at vertical height, z . By treating rotations of bundle lattice and filament grooves independently, we neglect small, position dependent corrections to ϕ' needed to maintain constant groove orientation in the $x - y$ plane. It can be shown that these corrections contribute to the bundle free energy density by a factor proportional to $C\Omega^4 R^2$, at higher-order in Ω than the in-plane linker shear cost.
- [35] The numerical values are derived with the Gaussian interpolation formula for f_{twist} and may differ slightly in the full model.